NAVAL POSTGRADUATE SCHOOL
Monterey, California

THESIS

Viscoelastic Fracture Characterization
of a Solid Propellant

by

Charles Miller Hertzler

Thesis Advisor: G.H. Lindsey

June 1972

Approved for public release; distribution unlimited.

Security Classification

DOCUMENT CONTROL DATA - R & D

(Security classification of title, body of abstract and indexing annotation must be entered when the overall report is classified)

1. ORIGINATING ACTIVITY (Corporate author)	2a. REPORT SECURITY CLASSIFICATION
Naval Postgraduate School Monterey, California 93940	Unclassified
	2b. GROUP

3. REPORT TITLE

Viscoelastic Fracture Characterization of a Solid Propellant

4. DESCRIPTIVE NOTES (Type of report and, inclusive dates)

Aeronautical Engineer; (June 1972)

5. AUTHOR(S) (First name, middle initial, last name)

Charles Miller Hertzler

6. REPORT DATE	7a. TOTAL NO. OF PAGES	7b. NO. OF REFS
June 1972	41	14

8a. CONTRACT OR GRANT NO.	9a. ORIGINATOR'S REPORT NUMBER(S)
b. PROJECT NO.	
c.	9b. OTHER REPORT NO(S) (Any other numbers that may be assigned this report)
d.	

10. DISTRIBUTION STATEMENT

Approved for public release; distribution unlimited.

11. SUPPLEMENTARY NOTES	12. SPONSORING MILITARY ACTIVITY
	Naval Postgraduate School Monterey, California 93940

13. ABSTRACT

Both analytical and experimental studies were conducted on a propagating crack in a viscoelastic material. By applying an extension of the "correspondence principle" the stress and displacement at the crack tip were found as functions of the crack tip stress intensity factor. An energy balance was made for the specimen which allowed this factor to be related to geometric and load parameters. Fracture characterization was then performed by experimentally relating the crack tip stress intensity factor to the crack velocity.

The theory was applied to solid propellant fracture tests; however, the dewetting behavior of the propellant was not accounted for by the theory.

DD FORM 1 NOV 65 1473 (PAGE 1)

S/N 0101-807-6811

Security Classification

A-31408

14. KEY WORDS	LINK A		LINK B		LINK C	
	ROLE	WT	ROLE	WT	ROLE	WT
Fracture						
Viscoelastic Fracture						
Propellant Fracture						

DD FORM 1 NOV 65 1473 (BACK)

S/N 0101-807-6821

A-31409

Viscoelastic Fracture Characterization of a Solid Propellant

by

Charles Miller Hertzler
Lieutenant, United States Navy
M.S., Naval Postgraduate School, 1971

Submitted in partial fulfillment of the
requirements for the degree of

AERONAUTICAL ENGINEER

from the

NAVAL POSTGRADUATE SCHOOL
June 1972

Author 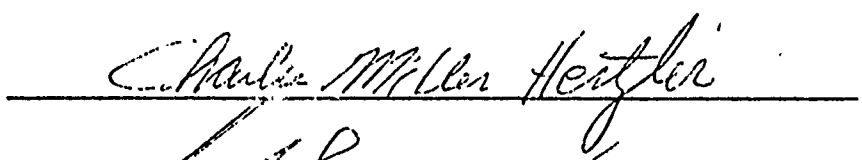

Approved by: 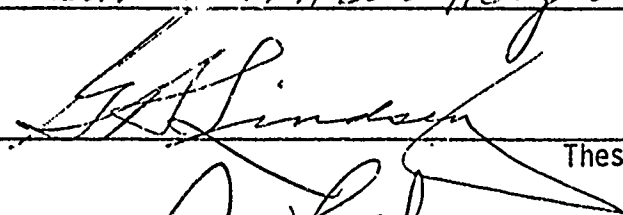
Thesis Advisor

Chairman, Department of Aeronautics

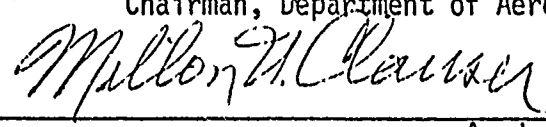
Academic Dean

TABLE OF CONTENTS

I. INTRODUCTION ---------- 5

II. THEORY ---------- 8

A. CRACK TIP STRESS AND DISPLACEMENT ---------- 8

B. ENERGY BALANCE ---------- 12

1. Reversibly Stored Energy ---------- 14

2. Energy Dissipated at the Crack Tip ---------- 15

3. Specific Specimen Geometry ---------- 18

C. ADDITIONAL RESULTS ---------- 20

D. TIME-TEMPERATURE SHIFT ---------- 21

III. EXPERIMENTAL RESULTS ---------- 22

A. CONSTANT STRESS CASE ---------- 22

B. CONSTANT DISPLACEMENT CASE ---------- 24

IV. DISCUSSION OF RESULTS ---------- 32

V. CONCLUSIONS ---------- 36

REFERENCES ---------- 37

INITIAL DISTRIBUTION LIST ---------- 39

FORM DD 1473 ---------- 40

ACKNOWLEDGEMENT

The author is indebted to United Technology Center, Sunnyvale, California, for supplying solid propellant and laboratory facilities used in this research. The helpful advice given by Mr. E. C. Francis, head of the Mechanical Properties Section, is gratefully acknowledged.

The contributions of Professor M. H. Bank as a second reader on this thesis are also acknowledged.

I. INTRODUCTION

In the elastic crack propagation problem, it is useful to define a crack tip stress intensity factor, K. This factor, which includes the effects of specimen loading and geometry, gives a measure of the stress concentration at the crack tip. As the load on a specimen containing a stationary crack is increased, K increases until a critical value is reached, whereupon the crack rapidly propagates. This critical value, K_c, is experimentally measured and found to be a material property.[1] A material may then be characterized by this constant, for if any combination of geometry and loading should produce K_c, crack propagation will occur.

For cracks in viscoelastic materials, Knauss and Mueller [Ref. 2] showed that in effect there is a certain minimum loading which will initiate crack propagation; that is, there is a loading below which the crack velocity is small enough to be considered equal to zero. However, the velocity of propagation will vary over a range of several orders of magnitude, increasing with increasing load. Thus the question to be answered in the viscoelastic fracture problem is not simply will the crack propagate, but rather at what velocity will it propagate. Knauss [Ref. 3] proposed that for a given viscoelastic material, $K(\dot{c})$ is a unique function, where $\dot{c}$ refers to the crack velocity. Therefore it is natural to experimentally characterize viscoelastic materials by this relation.

[1] The material property, K_c, is unique for most materials and geometries. However, there is a variation of K_c with initial crack length (usually small enough to be ignored) explained by consideration of the growth resistance curve as shown in Ref. 1.

A common method of obtaining viscoelastic solutions is to use the "correspondence principle." Lee [Ref. 4] showed that viscoelastic boundary value problems possess the property that an appropriate elastic solution in the Laplace transform domain may be inverted into the time domain to give the viscoelastic solution. However, this "correspondence principle" does not in general apply to problems where the boundary conditions are mixed and apply over regions which change with time.

Now looking at the problem of the propagating viscoelastic crack, note that the crack edge boundary condition immediately behind the crack tip is zero stress while the boundary condition on the extended line of propagation of the crack, immediately in front of the tip, is zero displacement. Propagation of the crack implies that portions of the boundary under zero displacement are continually changing into zero stress boundaries. Thus, the restriction on the "correspondence principle" mentioned above prohibits its application to this problem.

A different solution method has been used by Dietmann, Knauss and Mueller [Refs. 2,5,6,7] in their various studies of propagating cracks in viscoelastic materials. In all of these cases, the actual problem was approximated by one in which crack propagation was a step-wise process. The resulting solutions in all cases contained the length of the crack increment used in the step-wise process as a material property; however, this length does not physically exist in the actual problem and therefore seems to be only the result of the solution technique.

In the solution of the viscoelastic fracture problem developed in this paper, the "extended correspondence principle" will be used. This extension is due to Graham [Ref. 8] who extended the classic

"correspondence principle" to cover several cases where mixed boundary conditions applied over regions which changed with time. Using this extension, both the viscoelastic stress and displacement in the vicinity of the tip of a continuously propagating crack will be obtained as functions of the stress intensity factor, K. The remainder of the solution will consist of applying an energy balance to the specimen and relating K to the loading and geometric parameters of the specimen.

II. THEORY

Consider a thin, narrow sheet of isotropic, homogeneous, linear viscoelastic material loaded uniaxially by $\sigma_a(X,t)$ (where X refers to geometric coordinates and t to time) containing a continuously propagating center crack of length 2c(t) as shown in Figure 1.

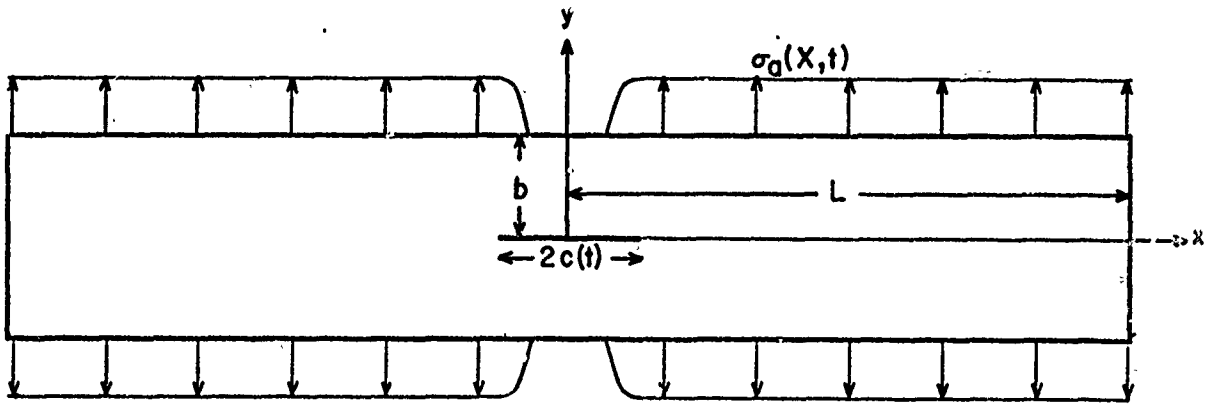

Figure 1. Specimen Geometry and Loading.

Assuming that the material is thermorheologically simple, the analysis for the stress intensity factor is made at a constant reference temperature, T_o. This solution will then be valid at any other temperature when appropriately shifted.

A. CRACK TIP STRESS AND DISPLACEMENT

In this analysis a knowledge of the work produced at the crack tip will be necessary. This further requires an evaluation of the stress and displacement fields in the vicinity of the moving crack tip, which is now undertaken.

If the sheet and loading are doubly symmetric, a single quadrant may be considered, as shown in Figure 2, where the lower right quadrant is removed and replaced by the stresses which act along the sheet's horizontal centerline.

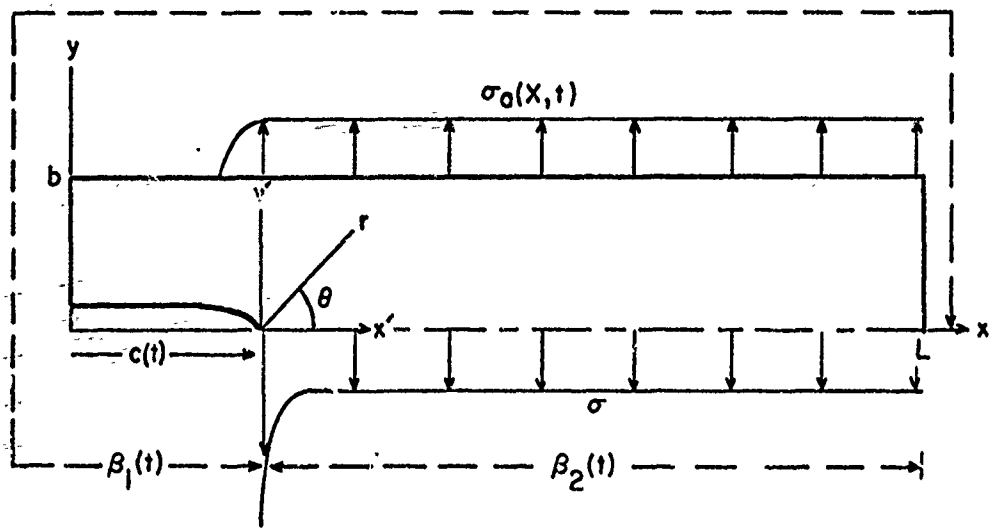

Figure 2. Single Quadrant of the Doubly Symmetric Specimen.

Let the entire boundary of the sheet be defined as β with $\beta_2(t)$ representing the uncracked portion of the x-axis and $\beta_1(t)$ representing the remaining boundary. Then $\beta = \beta_1(t) \cup \beta_2(t)$. The boundary conditions are:

$$\begin{aligned} \sigma_s(X,t) &= 0 && && \text{on } \beta \\ \sigma_n(X,t) &= \begin{cases} 0 & \text{on crack edge} \\ 0 & \text{on } x = 0,1 \\ \sigma_a(X,t) & \text{on } y = b \end{cases} && && \text{on } \beta_1(t) \\ u_n(X,t) &= 0 && && \text{on } \beta_2(t) \end{aligned} \qquad (1)$$

where u refers to displacement and the subscripts s and n respectively refer to normal and shear components. The boundary conditions of

Equation (1) meet the criteria of Graham's "extended correspondence principle."

However, to apply this correspondence, the elastic stresses and displacements in the vicinity of a stationary crack tip are needed. They have been found by Irwin [Ref. 9] to be:

$$\sigma_n = \frac{K_1}{\sqrt{2\pi\, r}} \cos\frac{\theta}{2}\left[1 + \sin\frac{\theta}{2}\sin\frac{3\theta}{2}\right] \tag{2}$$

$$u_n = \frac{K_1}{G}\sqrt{\frac{r}{2\pi}}\sin\frac{\theta}{2}\left[2 - 2\nu - \cos^2\frac{\theta}{2}\right] \tag{3}$$

where the subscript 1 on the stress intensity factor indicates that the crack is propagating in the opening mode as defined by Ref. 10.

Setting $\theta = 0$ in Equation (2) and $\theta = \pi$ in Equation (3) gives the stress and displacement, close to the tip, on $\beta_2(t)$ and $\beta_1(t)$ respectively. It is reasonable to assume that Equations (2) and (3) apply to slowly propagating cracks where the inertia effects are negligibly small in the equilibrium equation. Changing to an inertial coordinate system, where $x = c(t) + x'$ (refer to Figure 2) and assuming the incompessible case ($\nu = \frac{1}{2}$), the elastic stress and displacement in the vicinity of a slowly moving crack tip become the following:[2]

$$\sigma_n^e(X,t) = \frac{K_1(t)}{\sqrt{2\pi\,(x-c(t))}}\, h(\hat{t} - t) \qquad \text{on } \beta_2(t) \tag{4}$$

$$u_n^e(X,t) = \begin{cases} 2\sqrt{\frac{2}{\pi}}\,\frac{1}{E}\,K_1(t)\,\sqrt{c(t)-x}\;\; h(t-\hat{t}) & \text{on crack edge} \\ u_1^e(X,t) & \text{on } x = 0,1 \\ u_2^e(X,t) & \text{on } y = b \end{cases} \beta_1(t) \tag{5}$$

[2] In elastic theory, the stress intensity factor in these equations is the critical one, K_{1c}, since the crack is moving. However, in the viscoelastic case, with continuous propagation, this definition of the critical value loses its significance.

where superscript e refers to elastic solutions, $u_1^e(X,t)$ and $u_2^e(X,t)$ are elastic displacements which are functions of geometry and modulus, h(t) is the unit step function and $\hat{t}$ is the time at which the crack tip passed a point on the horizontal axis located at x.

Graham has shown that Equations (4) and (5) are the solutions to the viscoelastic problem in the Laplace transform plane if the elastic modulus is replaced by the transform modulus, $E \rightarrow pE_{rel}(p)$. Therefore, the field quantities of interest are:

$$\sigma_n^* (X,p) = \left[\frac{K_1(t)}{\sqrt{2\pi\,(x-c(t))}}\; h\,(\hat{t} - t) \right]^* \quad \text{on } \beta_2(t) \tag{6}$$

$$u_n^* (X,p) = 2\sqrt{\frac{2}{\pi}}\; \frac{1}{pE_{rel}(p)} \left[K_1(t) \sqrt{c(t) - x}\;\; h(t - \hat{t}) \right]^* \quad \text{on } \beta_1(t) \tag{7}$$

where: $\int_0^\infty e^{-pt} f(t)dt = [f(t)]^*$

Since $pD_{cr}(p) = 1/pE_{rel}(p)$, where D_{cr} refers to creep compliance, the viscoelastic solution inverts back into the time domain with the stress distribution identical to the elastic case and the displacement at the crack tip edge given by:

$$u_n (x,t) = 2\sqrt{\frac{2}{\pi}} \left\{ D_{cr}(t)\; K_1(0) \sqrt{c(0) - x}\;\; h(0-\hat{t}) + \int_0^t D_{cr}(t-\tau)\; \frac{\partial}{\partial \tau} \left[K_1(\tau) \sqrt{c(\tau) - x}\;\; h(\tau - \hat{t}) \right] d\tau \right\} \tag{8}$$

Since $h(0 - t) = 0$ and $h(\tau - \hat{t}) = 0$ for $\tau < \hat{t}$, Equation (8) may be rewritten as:

$$u_n (x,t) = 2\sqrt{\frac{2}{\pi}} \int_{\hat{t}}^t D_{cr}(t-\tau)\; \frac{\partial}{\partial \tau} \left[K_1(\tau) \sqrt{c(\tau) - x} \right] d\tau \tag{9}$$

Time $\hat{t}$ is seen to be equal to time t minus the time which it took for the crack to run between x and c(t), that is:

$$\hat{t} = t - \frac{c(t) - x}{\dot{c}_m} \tag{10}$$

where $\dot{c}_m$ is the mean velocity in the interval [x,c(t)]. Thus, time $\hat{t}$ accounts for the history which has affected the displacement at point x. Or to put it another way, the crack displacement at point x, at the present time t, has been creeping open ever since the crack tip passed that point at time $\hat{t}$.

The expressions for the stress and displacement, which have been found in this section, will allow the energy lost at the moving crack tip to be evaluated. Thus, the analysis now proceeds to an energy balance.

B. ENERGY BALANCE

An energy balance will now be applied to the entire specimen. First the specimen energies are defined as follows: W is the work input to the specimen by forces acting on the boundaries; I is the reversibly stored energy in the viscoelastic specimen; D is the energy which is dissipated throughout the specimen due to the viscous action of the material; finally, S is the energy which is dissipated at the crack tip in the creation of new surface area.

Neglecting heat and inertia terms, the First Law of Thermodynamics may be written:

$$W = I + D + S$$

The significant variables in the problem are c and t, thus the power equation becomes:

$$\left.\frac{\partial W}{\partial c}\right|_t \dot{c} + \left.\frac{\partial W}{\partial t}\right|_c = \left.\frac{\partial I}{\partial c}\right|_t \dot{c} + \left.\frac{\partial I}{\partial t}\right|_c + \left.\frac{\partial D}{\partial c}\right|_t \dot{c} + \left.\frac{\partial D}{\partial t}\right|_c + \left.\frac{\partial S}{\partial c}\right|_t \dot{c} + \left.\frac{\partial S}{\partial t}\right|_c$$

Rearranging terms the following equation is obtained.

$$\left[\frac{\partial W}{\partial c} - \frac{\partial I}{\partial c} - \frac{\partial D}{\partial c} - \frac{\partial S}{\partial c}\right]_t \dot{c} = \left[-\frac{\partial W}{\partial t} + \frac{\partial I}{\partial t} + \frac{\partial D}{\partial t} + \frac{\partial S}{\partial t}\right]_c \qquad (11)$$

The left hand side of Equation (11) may be thought of as describing the elastic behavior of the viscoelastic speciman (that behavior which is independent of time) while the right hand side describes the viscoelastic (time dependent) behavior. However, $\left.\frac{\partial S}{\partial t}\right|_c = 0$ since there is no mechanism to create energy S. Thus, for a fixed crack length, the first law becomes W = I + D and the right hand brackets of Equation (11) sums to zero. Also, viscous dissipation is physically an energy which must occur over finite time, thus in the left hand side of Equation (11):

$$\left.\frac{\partial D}{\partial c}\right|_t = 0$$

Therefore if time is held constant, Equation(11) becomes:

$$\left[\frac{\partial W}{\partial c} - \frac{\partial I}{\partial c} - \frac{\partial S}{\partial c}\right]_t = 0 \qquad (12)$$

Of the energies which appear in Equation (12), W is the most directly evaluated. It is simply the energy produced by the applied force, σ_a, moving through the displacement at the boundary. The remaining energies of Equation (12) will now be considered in detail.

1. Reversibly Stored Energy

To further clarify the definition of I at any time t, consider the following. Uniaxial viscoelastic behavior can be modeled by the three-element mechanical model consisting of a Maxwell element and a spring loaded in parallel as shown in Figure 3. The short-time spring constant for the model is $E_g = E + E_r$ where $E >> E_r$. The spring constants of the model correspond to the slopes in a stress-strain plot while model force and displacement correspond respectively to viscoelastic stress and strain.

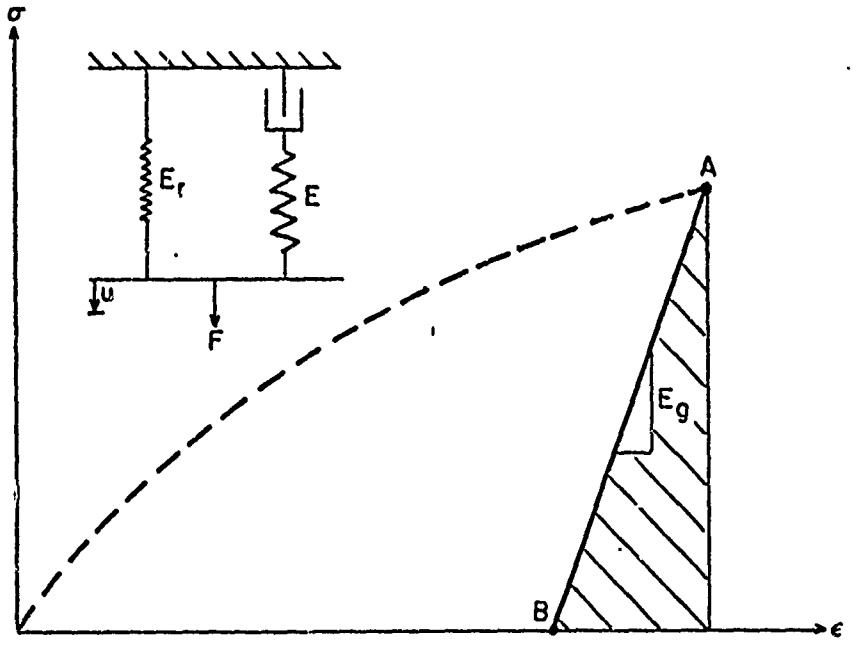

Figure 3. Stress-Strain Plot and Mechanical Model for Viscoelastic, Reversibly Stored Energy.

Consider the loaded viscoelastic body (model) at any time t (point A). Allow an instantaneous relaxation, thus losing no energy in viscous dissipation in the model dashpot, and calculate the energy

released. Since this is a conservative process, the energy released will be the reversibly stored energy.

The relaxation occurs with the short-time modulus to a point of zero stress (point B). The energy released per unit volume is the area under the path AB in the stress-strain plot or:

$$\frac{I}{VOL} = \frac{1}{2} \frac{\sigma^2(t)}{E_g}$$

Comparing this to the strain energy of a uniaxially loaded elastic body:

$$\frac{U}{VOL} = \frac{1}{2} \frac{\sigma^2}{E}$$

the following correspondence may be made between elastic strain energy and internal energy in specimens of identical geometry which are loaded uniaxially.

$$\begin{aligned} & U \rightarrow I \\ \text{if} \quad & E \rightarrow E_g \\ \text{and} \quad & \sigma \rightarrow (t) \end{aligned} \tag{13}$$

2. Energy Dissipated at the Crack Tip

The change in energy S with respect to length, at the crack tip, required in equation (12), is now evaluated. Holding $t = t_c$, allow a small propagation of α (see Figure 4). Since this is for constant time, the behavior of the viscoelastic material is elastic and the evaluation technique used by Irwin [Ref. 9] for elastic materials may be applied. Thus, the energy lost in this process is:

$$\Delta S = \frac{1}{2} \int_0^{\alpha} u_{n_{max}} \sigma_{n_{max}} \, dx'$$

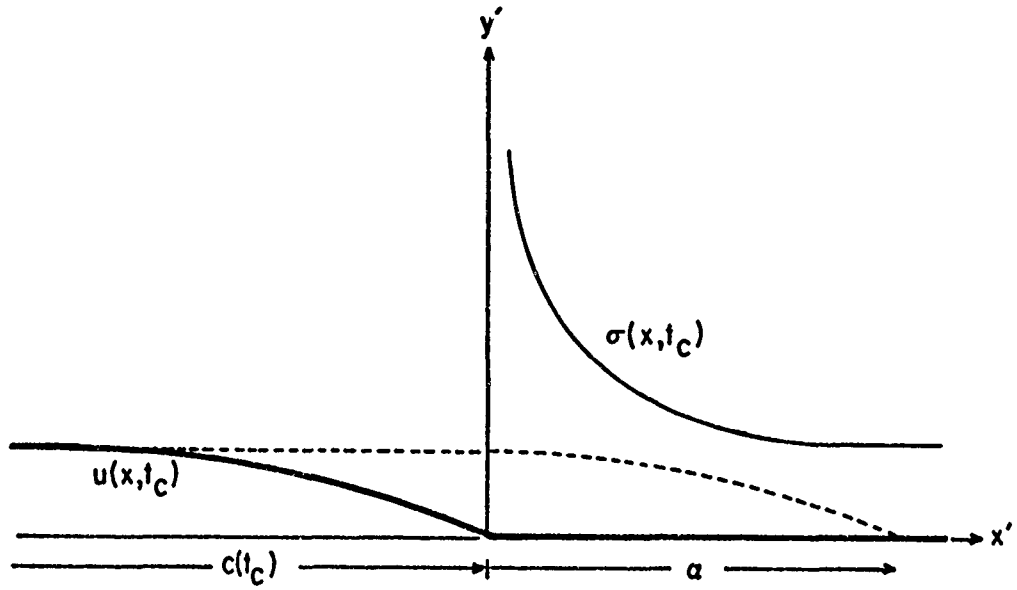

Figure 4. Crack Tip for Incremental Propagation, α, at $t = t_c$.

Substituting for the maximum values of displacement and stress, this becomes:

$$\Delta S = \frac{1}{2} \int_0^{\alpha} u_n (x' - \alpha, t_c)\, \sigma_n (x', t_c)\, dx'$$

or in inertial coordinates:

$$\Delta S = \frac{1}{2} \int_{c(t_c)}^{c(t_c)+\alpha} u_n(x-c(t_c) - \alpha, t_c)\, \sigma_n (x - c(t_c), t_c)\, dx \qquad (14)$$

Equation (14) requires that the displacement of Equation (9) be translated by $x = \alpha$. Note that the lower limit on the integral of Equation(10), which is a function of position, thus changes to:

$$t_c + \frac{x - c(t) - \alpha}{\dot{c}_m} = \hat{t} - \frac{\alpha}{\dot{c}_m} \qquad (15)$$

With this change in limits, the displacement, Equation (9), and the stress, Equation (4), are substituted into Equation (14) to give:

$$\Delta S = \frac{K_1(t_c)}{\pi} \int_{c(t_c)}^{c(t_c)+\alpha} \int_{\hat{t}-\frac{\alpha}{\dot{c}_m}}^{t_c} \frac{D_{cr}(t_c-\tau)}{\sqrt{x-c(t_c)}} \frac{\partial}{\partial\tau} \left[K_1(\tau)\sqrt{c(\tau) - x + \alpha}\right] d\tau dx \qquad (16)$$

Consider the compliance in Equation (16). At the upper limit in time it becomes $D_{cr}(0)$ while at the lower limit it is:

$$D_{cr}\left(\frac{c(t_c) - x + \alpha}{\dot{c}_m}\right)$$

which is a function of x. Now evaluating at the upper limit in x, it again is $D_{cr}(0)$ while at the lower limit is becomes $D_{cr}(\alpha/\dot{c}_m)$. Thus since α is small, the compliance may be approximated by the constant value, $D_{cr}(0)$. The integrand in time is now a perfect derivative and Equation (16) becomes:

$$\Delta S = \frac{K_1(t_c)}{\pi} D_{cr}(0) \int_{c(t_c)}^{c(t_c)+\alpha} \frac{1}{\sqrt{x-c(t_c)}} \left[K_1(t_c)\sqrt{c(t_c) - x + \alpha} - K_1(\hat{t} - \tfrac{\alpha}{\dot{c}_m})\sqrt{c(\hat{t} - \tfrac{\alpha}{\dot{c}_m}) - x + \alpha}\right] dx \qquad (17)$$

Consider the integrand of Equation (17) which is evaluated at any x for which $c(t_c) \le x \le c(t_c) + \alpha$. Choosing x, $c(\hat{t} - \frac{\alpha}{\dot{c}_m})$ is seen to be equal to the crack length at the time it passed x minus the length of time it took to propagate through a distance α at its mean velocity, $\dot{c}_m$. In other words, $c(\hat{t} - \frac{\alpha}{\dot{c}_m})$ is equal to $x - \alpha$ and the second term in

the brackets vanishes. Now the time dependence in this energy has been evaluated and Equation (17) may be conveniently written in local coordinates as:

$$\Delta S = \frac{K_1^2(t_c)}{\pi} D_{cr}(0) \int_0^{\alpha} \sqrt{\frac{\alpha - x'}{x'}}\, dx'$$

which when integrated becomes:

$$\Delta S = \frac{K_1^2(t_c)}{2} D_{cr}(0)\, \alpha$$

Since α is small, the change in S with respect to c is:

$$\frac{\partial S}{\partial c} \simeq \frac{\Delta S}{\alpha} = \frac{K_1^2(t)\, D_{cr}(0)}{2} \tag{18}$$

where the subscript on t has been dropped since t_c was a typical time.

3. Specific Specimen Geometry

At this point, the energies required in Equation (12) have been defined or evaluated. However, since W and I depend on the particular geometry and loading, the evaluation for these energies has been only general. A specific case is shown in Figure 6 where the applied load, $\sigma_a(X,t)$, is:

$$\sigma_a(x, \pm b, t) = \begin{cases} \sigma_a & \text{for } x \geq c(t) \\ 0 & \text{for } x < c(t) \end{cases} \tag{19}$$

The strains in the specimen may be thought of as a superposition of the uniaxial strain for $x \geq c(t)$ and the strain produced by the stress field in the vicinity of the crack tip. Since the uniaxial displacement of the boundary edge is $\varepsilon(t)b$, choosing b sufficiently large will make this displacement of higher order than that produced on the boundary by the stress field at the crack tip. Thus holding

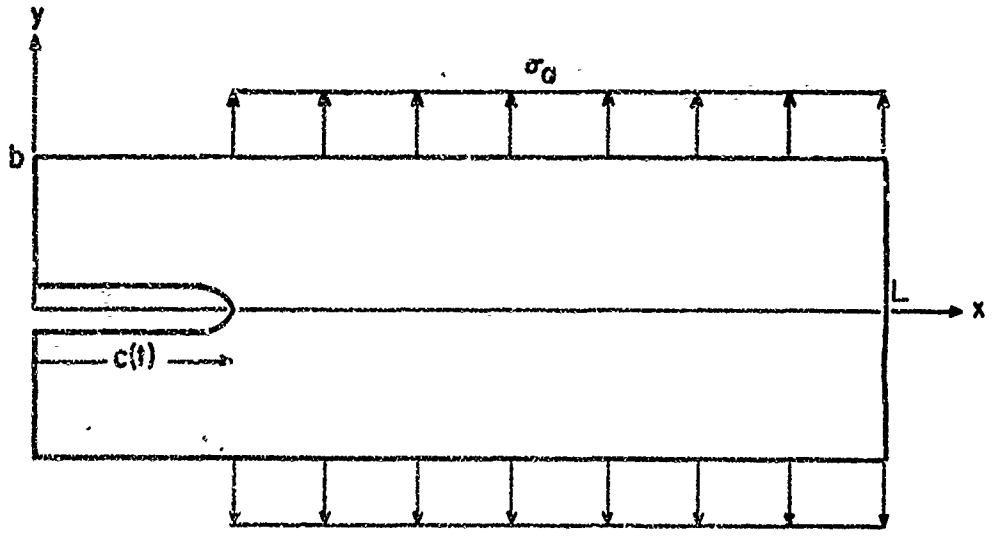

Figure 5. Specimen Geometry and Loading.

time constant and allowing an incremental propagation of dc, while removing load from the boundary as specified by Equation (19), produces negligible displacement, hence negligible work at the boundary. Therefore:

$$\left.\frac{\partial W}{\partial c}\right|_t \simeq 0 \tag{20}$$

For this specimen, if the uncracked length l - c(t) is maintained large enough so that a strip at the right hand edge is under uniaxial stress, that is, unaffected by the crack tip stress field, Ref. 11 gives the change in the elastic strain energy as:

$$\left.\frac{\partial U}{\partial c}\right|_t \simeq -\frac{\sigma^2}{E} b \tag{21}$$

Thus by applying Equation (13):

$$\left.\frac{\partial I}{\partial c}\right|_t = -\frac{\sigma_a^2}{E_g} b \tag{22}$$

Substituting Equations (18), (20) and (22) into Equation (12), noting that now surface energy is released from two surfaces and that $\mathcal{E}_g = 1/D_{cr}(0)$, gives:

$$K_1 = \sigma_a \sqrt{b} \tag{23}$$

Note that since σ_a is constant, K_1 is a constant. This result is identical to that which is obtained in the elastic case.

C. ADDITIONAL RESULTS

Lindsey [Ref. 11], applying Graham's "extended correspondence principle," transformed the elastic expressions for stress intensity factors directly into the viscoelastic case. His results agree with Equation (23) and include the additional case of a strip with displacement boundary conditions under a constant displacement, u_a (see Figure 6). (Uncracked specimens of this geometry are commonly used in the propellant industry and are referred to as "biaxial strips" since they are in a state of biaxial stress.) Lindsey's solution is:

$$K_1 = \sigma(t) \sqrt{\frac{3}{4} b} \tag{24}$$

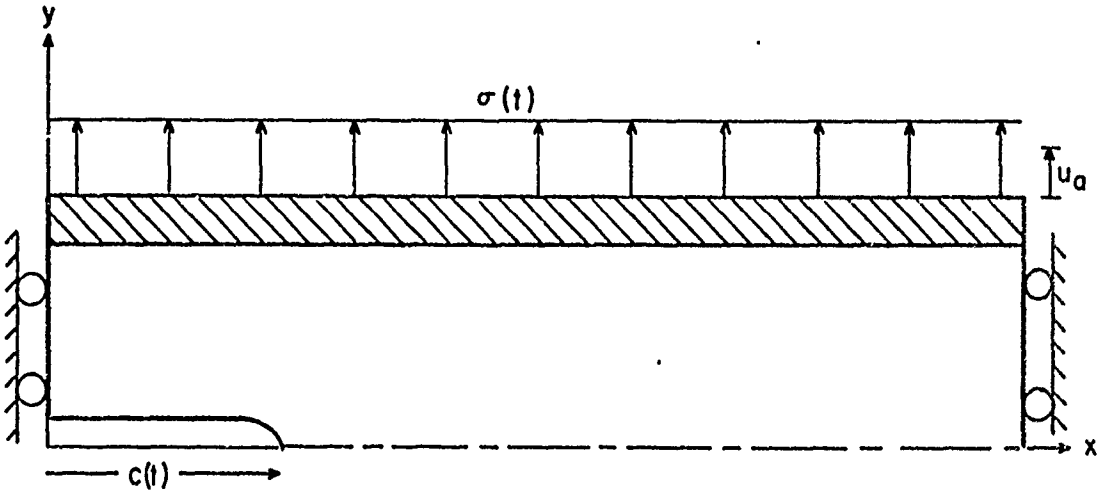

Figure 6. Cracked Biaxial Strip.

D. TIME-TEMPERATURE SHIFT

The expressions for $K_I(t)$, Equations (23) and (24) are for a constant reference temperature, T_o. Since the viscoelastic material was assumed to be thermorheologically simple, Ref. 12 shows that the modulus, hence the stress, may be shifted from any temperature, T, to the value at T_o by multiplying it by the factor $T_o \rho_o / T \rho$, where ρ is the material density. The time scale is corrected by dividing it by a time-temperature shift factor, a_T. Since $\rho \simeq \rho_o$, the expression for the stress intensity factor become:

$$K_I\left(\frac{t}{a_T}\right) = \frac{T_o}{T} \sigma_a \left(\frac{t}{a_T}\right) \sqrt{b} \qquad \text{stress B.C.} \qquad (25)$$

$$K_I\left(\frac{t}{a_T}\right) = \frac{T_o}{T} \sigma \left(\frac{t}{a_T}\right) \sqrt{\frac{3}{4} b} \qquad \text{disp. B.C.} \qquad (26)$$

These expressions can now be used to guide experimental measurements of $K_I(t/a_T)$. For, in light of the previous discussion concerning the relationship between K_I and $\dot{c}$, laboratory measurements of these two parameters in fracture tests will constitute a viscoelastic fracture characterization of the material.

III. EXPERIMENTAL RESULTS

Experimental testing was conducted on a CTPB solid propellant. This filled material consisted of solids (oxidizer) comprising approximately 85% of the total volume, bonded in a rubbery (fuel) matrix.

A. CONSTANT STRESS CASE

The specimen configuration to achieve the stress boundary conditions of Figure 5 is shown in Figure 7. The specimen was cut from samples designed for use in biaxial tests with a gage length of 1.0 inch and thickness of 0.1 inch. The wooden tabs were segmented with saw cuts which stopped in the adhesive bond just short of the propellant.

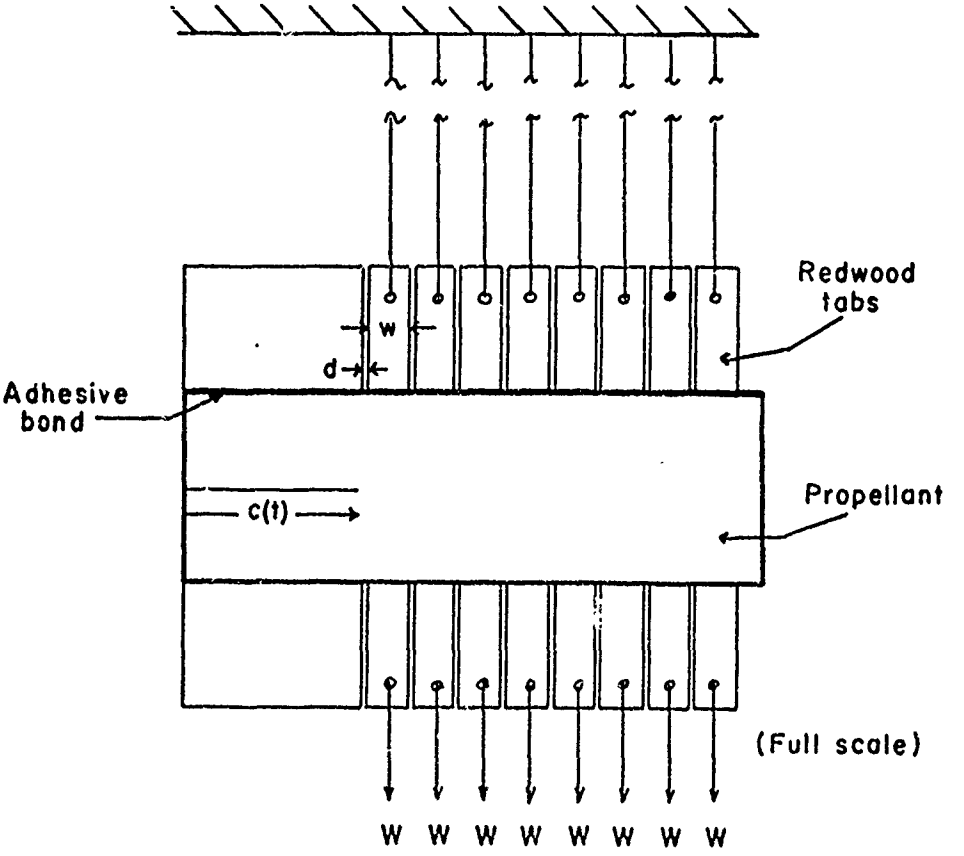

Figure 7. Specimen Configuration for Stress Boundary Conditions.

(To penetrate through the bond into the propellant would have created a stress riser and a point of probable crack initiation.) The width, w, ideally would be very small, allowing shear-free edges; however, practical considerations forced a width of w = 0.25 inch.

Initial experiments, with the right-hand edge of the propellant flush with the wooden tab edge, showed that soon after loading a fast running crack would initiate at a local defect along the right edge of even a carefully cut specimen. Adding a 1/8 inch unloaded length reduced the stress along this edge and eliminated the problem. To compensate for this departure from uniform stress at the right hand edge and yet still meet the restriction leading to Equation (21), $c(t)_{max}$ was limited to 2.0 inches.

The thickness of the saw cuts in the wooden tabs was large enough to allow unrestrained ε_x, or $d/w \geq \varepsilon_{x\ max}$. The upper segments were individually suspended and the lower segments were individually loaded by weights W. An initial crack of one inch was cut with a razor blade.

A specimen was tested by applying all loads at t = 0. The length of the propagating crack, c(t), was measured with an optical comparator. As the crack passed a segment, the weight on that segment was removed in proportion to the width of the segment traversed by the crack. The tests were conducted in an environmental chamber with the relative humidity less than 30%, at six temperatures ranging from 15°F to 85°F.

The stress intensity factor for each test was calculated by using Equation (25), assuming $a_T = 1$, and plotted on a graph of stress intensity factor versus crack velocity, for each specific testing temperature (see Figures 8 through 13). In this way the shift due to temperature, in the ordinate, was accounted for. However, complete

shifting of the function required that a_T be known. This was obtained graphically by shifting the curves for various temperatures along the abscissa, relative to the curve at T_0, so that a continuous function was obtained. The resulting characterization curve is shown in Figure 14, where T_0 = 70°F.

B. CONSTANT DISPLACEMENT CASE

Additional tests were conducted on cracked biaxial strip specimens. Though the ends were free, rather than restrained as shown in Figure 6, the long length relative to the width allowed the actual specimen to closely approximate the theoretical one. The strips were six inches in length, one inch in width (2b) and 1/10 inch thick. Redwood tabs bonded to the horizontal edges allowed for gripping. An initial crack of 0.75 inch was cut, as suggested by Mueller [Ref. 7]. As before, the length of the propagating crack was measured as a function of time with an optical comparator.

The testing was performed with the apparatus which was used for similar tests on solithane, as described in Ref. 13. Briefly this consisted of an Instron Universal Testing machine equiped with special jaws to clamp the specimen and apply displacement u_a while maintaining the upper and lower boundaries parallel. The displacement was applied at rates ranging from one inch/minute for low temperatures to five inches/minute at the high temperatures. A conditioning chamber allowed the tests to be conducted at the same specific temperatures as in the previous case.

Using Equation (26), K_1 was calculated and plotted in Figures 8 through 13. Shifting was performed as in the previous case, with T_0 = 70°F, and the master characterization curve plotted in Figure 14.

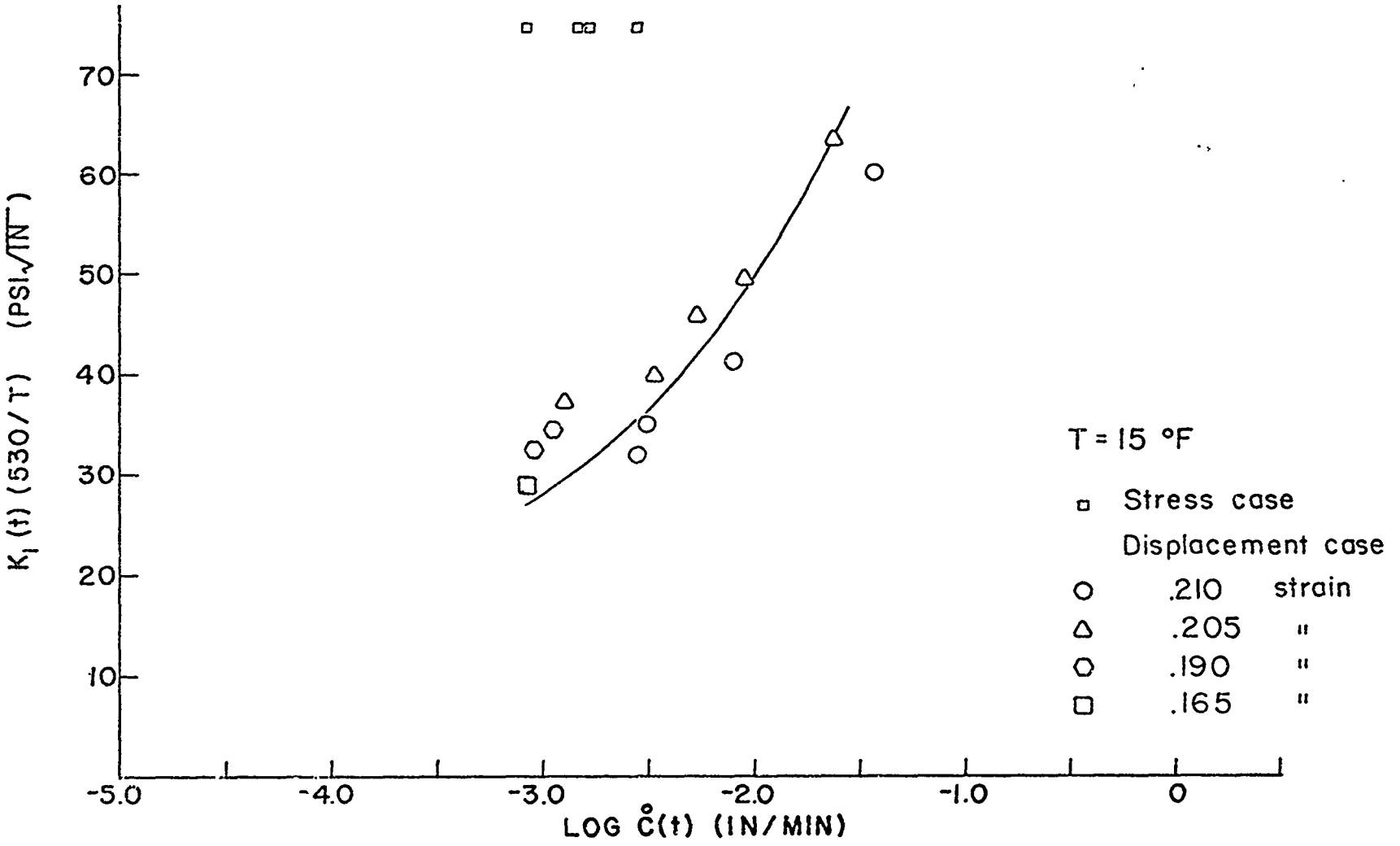

FIGURE 8 PROPELLANT FRACTURE CHARACTERIZATION CURVE FOR 15 °F

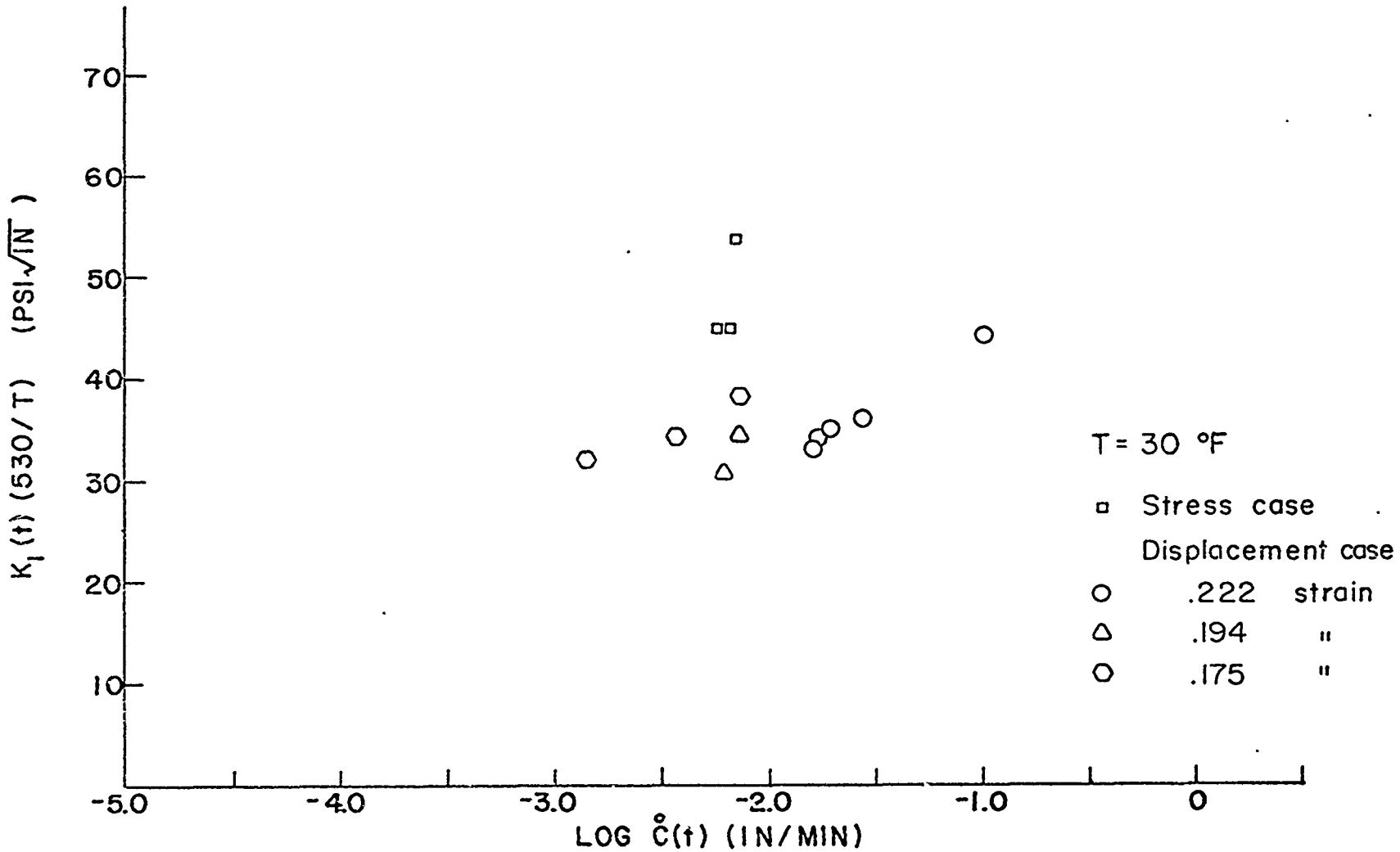

FIGURE 9 PROPELLANT FRACTURE CHARACTERIZATION CURVE FOR 30 °F

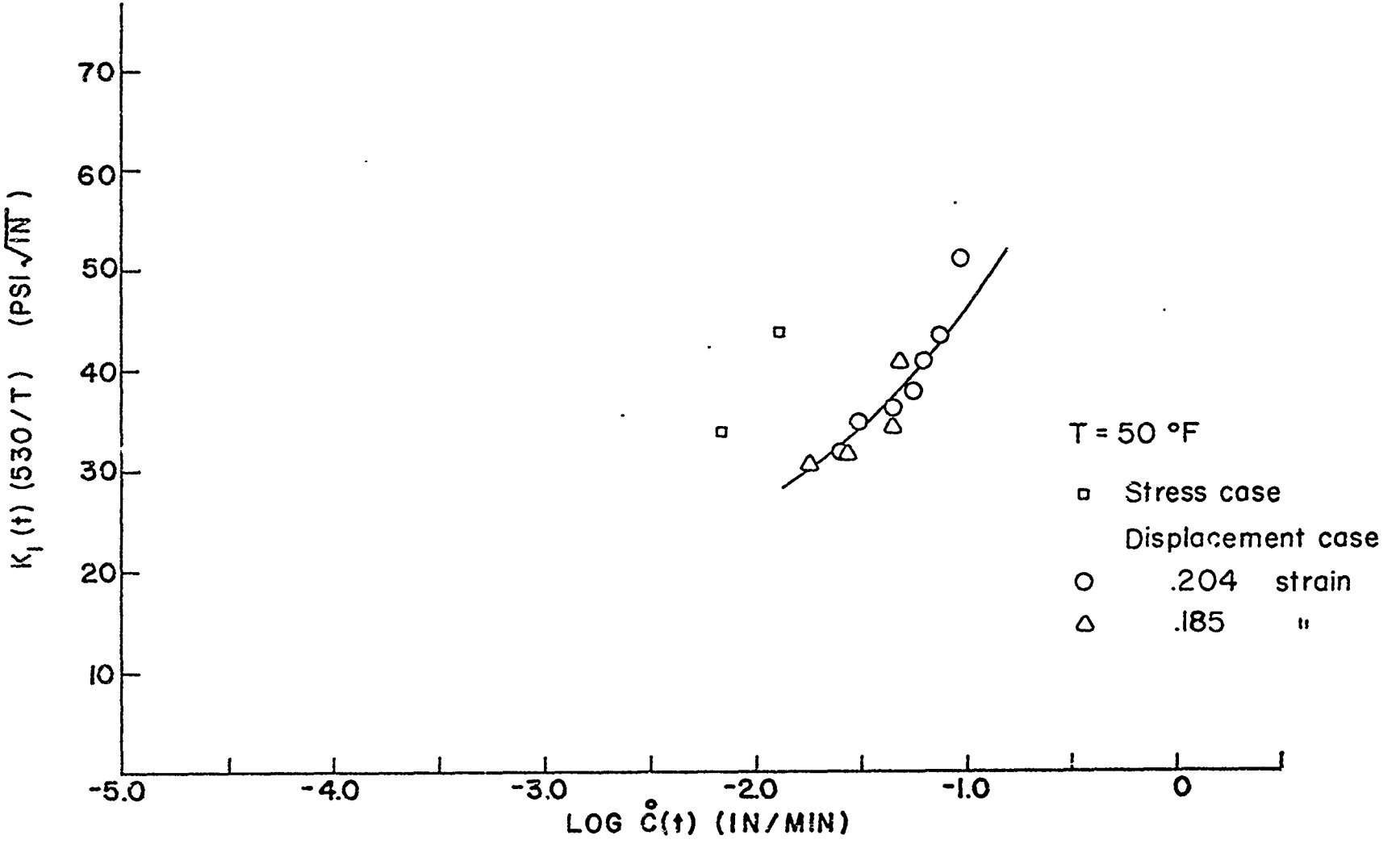

FIGURE 10 PROPELLANT FRACTURE CHARACTERIZATION CURVE FOR 50 °F

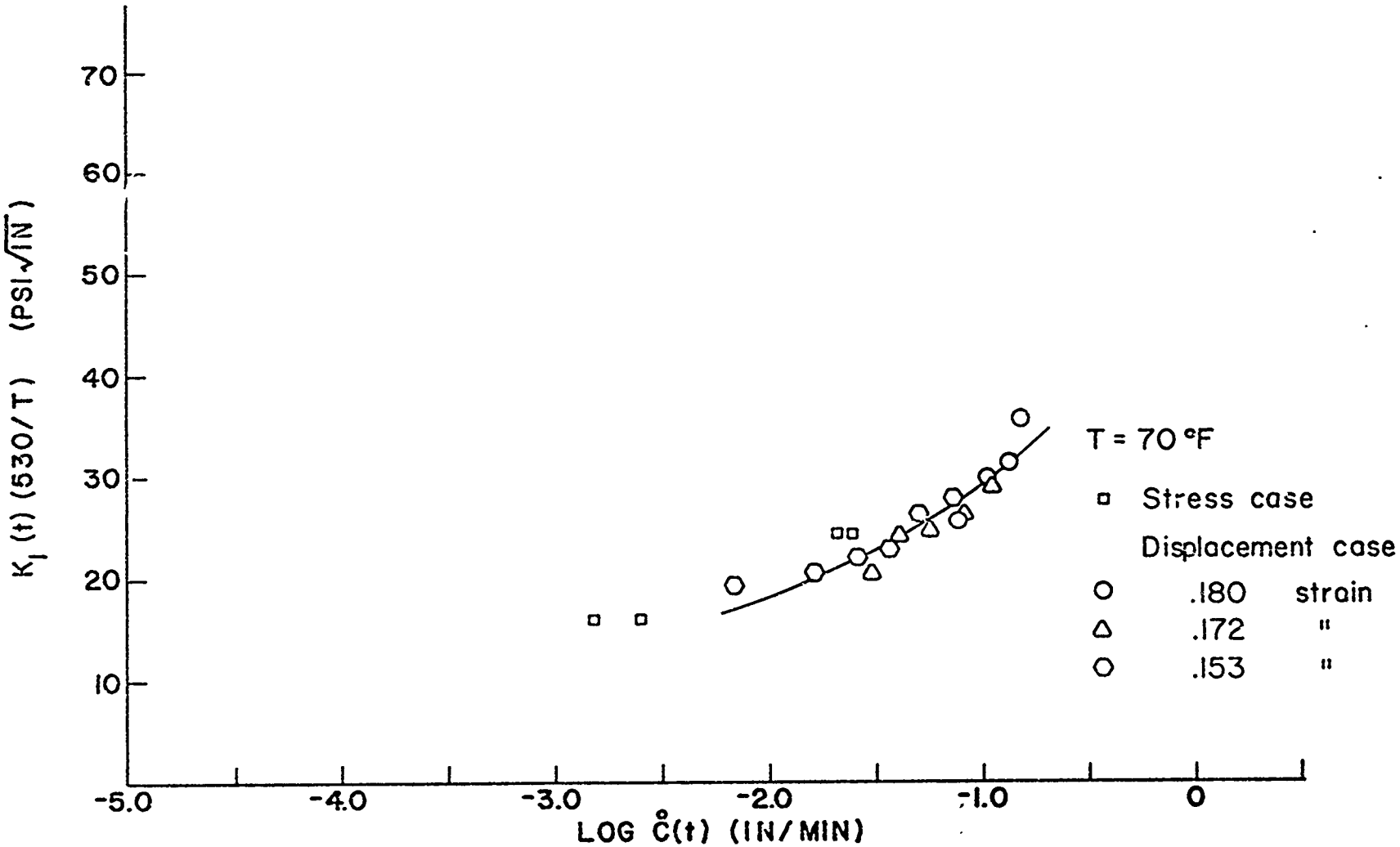

FIGURE 11 PROPELLANT FRACTURE CHARACTERIZATION CURVE FOR 70 °F

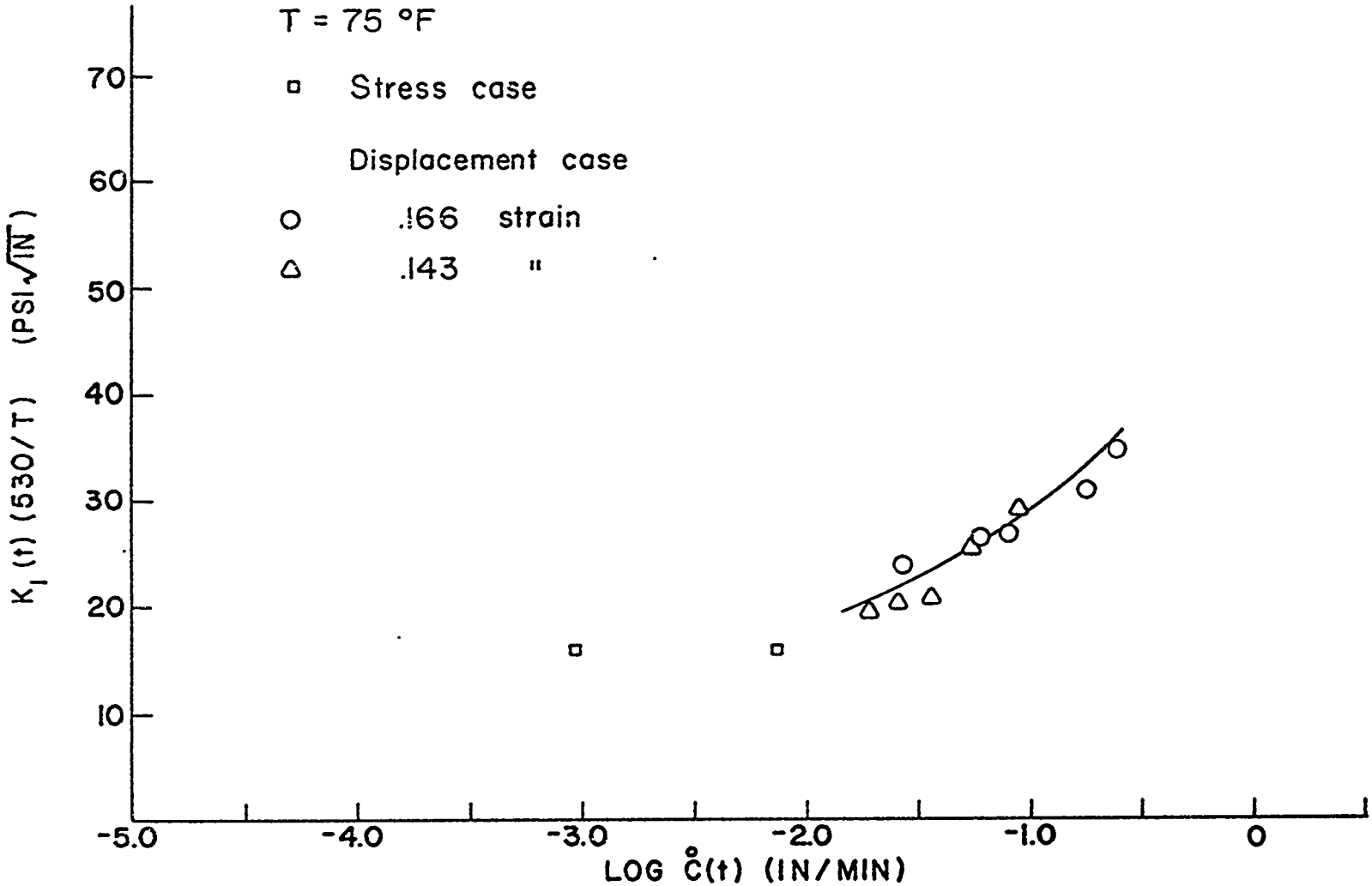

FIGURE 12 PROPELLANT FRACTURE CHARACTERIZATION CURVE FOR 75 °F

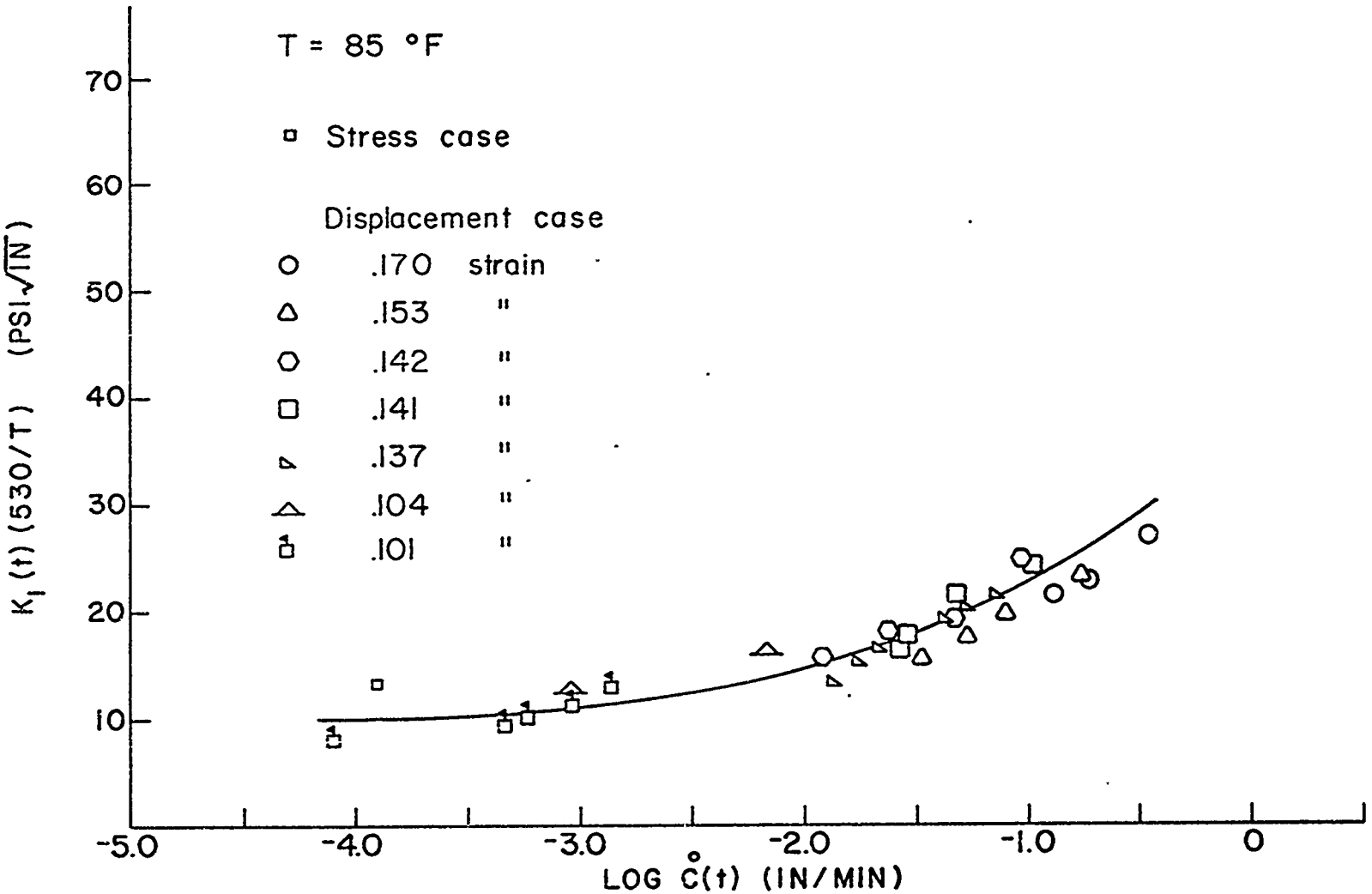

FIGURE 13 PROPELLANT FRACTURE CHARACTERIZATION CURVE FOR 85 °F

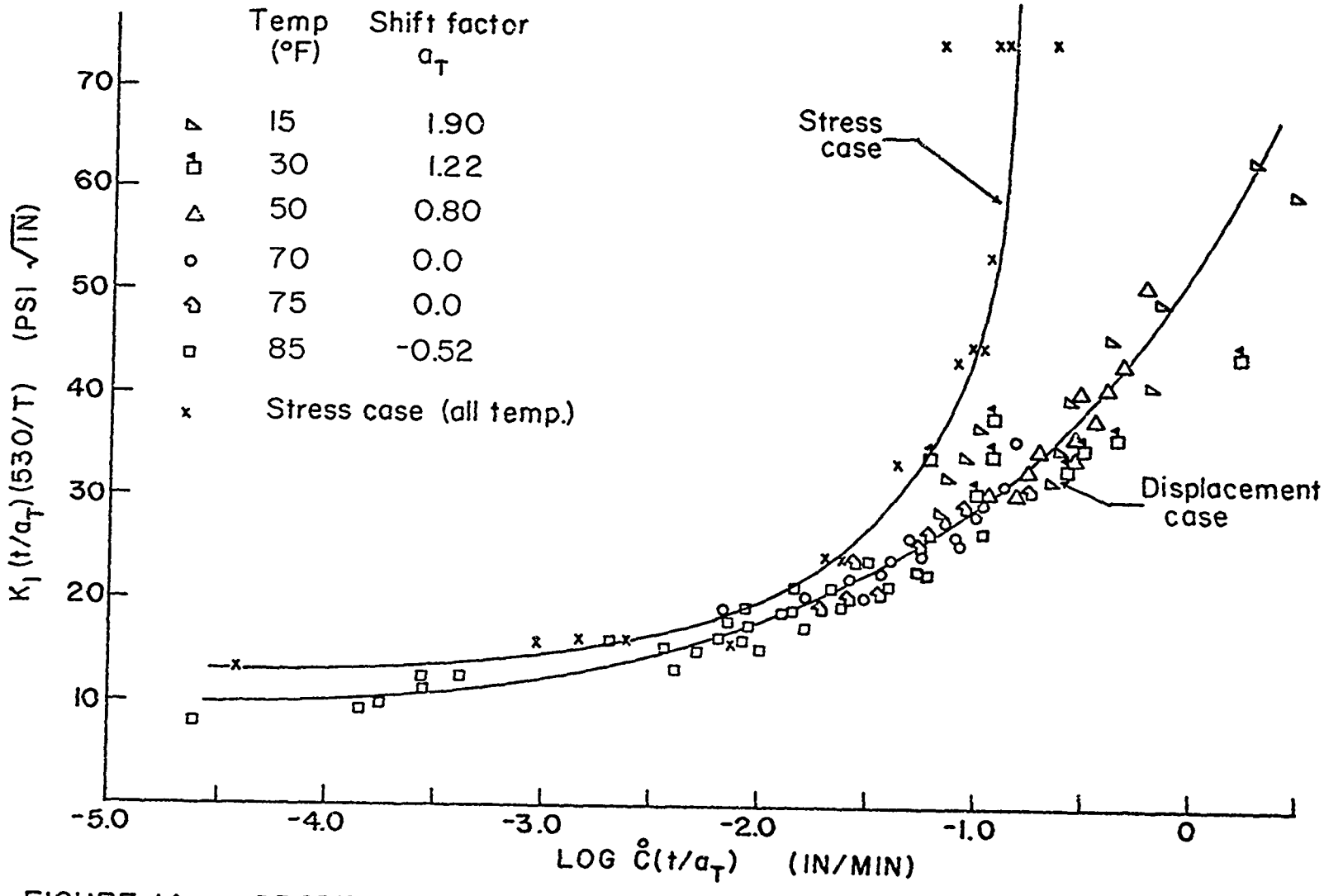

FIGURE 14 PROPELLANT FRACTURE CHARACTERIZATION MASTER CURVE

IV. DISCUSSION OF RESULTS

In the stress boundary condition case, the crack tip stress intensity is constant. This constant stress intensity should produce a constant velocity crack, a fact which was verified in these experiments. Therefore, each sample tested, for a given loading and temperature, produced a unique point on a plot of $K_I(\dot{c})$.

However, for the displacement boundary condition case, since the stress relaxes, the crack will decelerate until E_r (rubbery modulus) is reached. For the propellant tested, this relaxation time was on the order of a year. Therefore, for all experiments of this case, the crack was constantly decelerating. Thus $K_I(\dot{c})$ was a continuous function and in this study was shifted more readily than the stress data, since for the later case, limited samples precluded enough testing to obtain a well defined function for each temperature. For this reason the shift factors obtained in the displacement case were used in the stress case to shift the data to the master curve shown in Figure 14.

The theory of Section II considered a purely viscoelastic material. However, the solid propellant was a filled material, which when loaded, exhibits the additional mechanism of dewetting. (Dewetting is the breaking of bonds between solid filler particles and the rubbery matrix.) Wood [Ref. 14] has shown that propellant dewetting is not a rate process, rather it occurs upon initial application of stress. This behavior has a significant bearing on the experimental results obtained in this study as will now be shown.

In both cases tested, the measured load parameter was stress, thus automatically accounting for the modulus relaxation in the displacement

case. However, the two stress histories were quite different as shown in Figure 15. In the stress case, stress was constant while in the displacement case there was an initial extremely high stress which continually relaxed.[3]

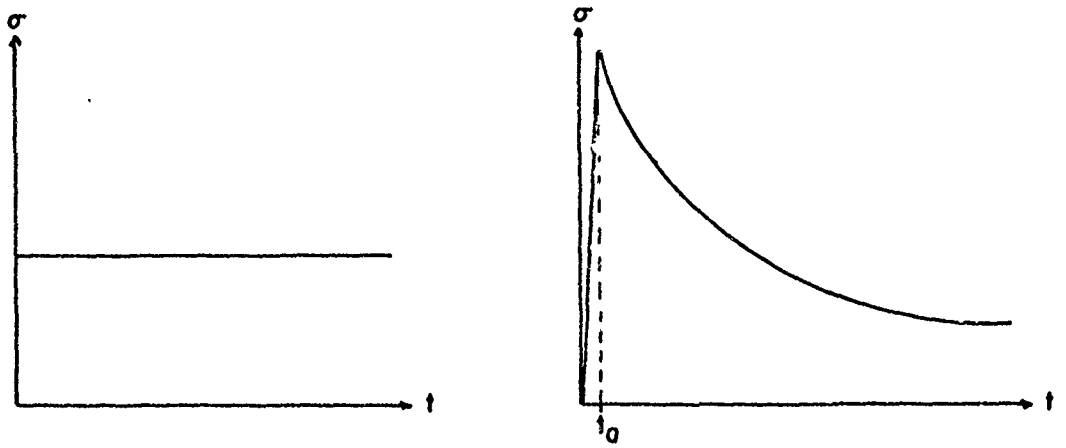

Constant Stress — Constant Displacement

Figure 15. Stress Histories.

Thus a sample tested in the stress case exhibited minimum dewetting because of its history of constant stress. However, in the displacement case, for a corresponding stress at $t \geq 10t_a$ (where t_a is the time required to apply the load) much more dewetting had occurred due to the initial high stress. Consequently the crack propagated through a material which had been significantly altered from that in the stress case. The propagating crack had fewer bonds to break per unit area, compared with the stress case, and accordingly its velocity was as much

[3]The theory of this paper does not account for any transients, rather considers only step loading. However, the application of the loading in the displacement case required finite time. Therefore, data taken for this case were taken at $t \geq 10t_a$ assuming that at this time, any effects of the loading method had died out.

as two orders of magnitude higher. This produced significantly different characterization curves for the two cases as shown in Figure 14.

Since dewetting produces microscopic voids in the material, stiffness is reduced as dewetting increases. Using this fact, the increased dewetting of the displacement case was verified in preliminary tests at 15°F. In these tests, for identical stress and time, the modulus in the displacement case was one-half that of the stress case.

In an attempt to reduce the initial high stress peak in the displacement case, thus reducing the dewetting, additional preliminary tests at 15°F were conducted. The maximum stress was limited to that which produced stress intensity factors comparable with those of the stress case for the same temperature. Equivalent moduli showed that the amount of dewetting was in fact equivalent. However, as soon as the displacement rate was stopped, the stress relaxed due to $E_{rel}(t)$. Thus even if the crack propagated at the same velocity as in the stress case (approximately 0.1 inch per hour) relaxation of the driving stress decelerated the crack to zero velocity over distances too small to be accurately measured. Thus, no additional characterization data were obtainable with this loading method.

The accuracy of the measured velocity in the stress case was considered superior to that of the displacement case, especially for low velocities. For in the displacement case, c(t) had to be measured over relatively short periods of time to obtain an accurate crack propagation function. (Velocity was obtained by graphically measuring the slope of this function.) As c(t) became small, $\Delta c(t)$ for the time interval

mentioned above also became small. Thus, because the experimental crack propagation was irregular due to inhomogeneities in the propellant, the actual velocity was obscured as those irregularities approached the magnitude of $\Delta c(t)$. However, in the stress case, $\dot{c}(t)$ was a constant and $\Delta c(t)$ could be measured over large time intervals.

The scatter in the characterization curves is due to the inaccuracies mentioned above for the displacement case and also to the inhomogeneous nature of a highly filled viscoelastic material such as propellant. By comparison, similar characterization of solithane, an unfilled and relatively more homogeneous material, by Francis et. al. [Ref. 13] showed significantly less scatter.[4]

Referring to the characterization curves, in both cases there appears to be a K_1 critical below which a crack will not propagate. Again for both cases, especially apparent in the stress case, there appears to be a maximum velocity of propagation; however these maximum velocities are somewhat misleading. Preliminary tests showed that at very high loads the failure was general and catastropic, initiated at voids and other stress risers throughout the specimen as well as at the crack tip.

[4]Solithane at room temperature has a relaxation time of less than one minute. Thus, though tested for the displacement case, essentially constant velocity crack propagation in these tests allowed the additional advantage of increased accuracy of the measured crack propagation function for reasons mentioned above.

V. CONCLUSIONS

The theory presented in this paper permits fracture characterization of a viscoelastic material to be made. However, for a filled viscoelastic material such as a solid propellant, dewetting behavior affects the crack velocity. (The stress boundary condition case is the limit case of minimum dewetting.) Additional theory is necessary to account for dewetting. This theory would then be expected to provide for a superposition of the displacement characterization curve upon the stress characterization curve (See Figure 14).

REFERENCES

1. Defense Metals Information Center Memorandum 252, Concepts in Fail-Safe Design of Aircraft Structures, March 1971.

2. Knauss, W.G. and Mueller, H.K., "Crack Propagation in a Linearly Viscoelastic Strip, " Journal of Applied Mechanics, p. 483, June 1971.

3. Knauss, W.G., "Stable and Unstable Crack Growth in Viscoelastic Media," Transactions of the Society of Rheology, v. 13:3, p. 291, 1969.

4. Lee, E.H "Stress Analysis in Visco-Elastic Bodies," Quarterly of Applied Mathematics, v. 13, p. 183, 1955.

5. Knauss, W.G., "Delayed Failure - The Griffith Problem for Linearly Viscoelastic Materials," International Journal of Fracture Mechanics, v. 6, no. 1, p. 7, March 1970.

6. Dietmann, H. and Knauss, W.G., "Crack Propagation Under Variable Load Histories in Linearly Viscoelastic Solids," International Journal of Engineering Science, v. 8, p. 643, 1970.

7. NASA CR-1279, Stable Crack Propagation in a Viscoelastic Strip, by H.K. Mueller, March 1969.

8. Graham, G.A.C., "The Correspondence Principle of Linear Viscoelasticity Theory for Mixed Boundary Value Problems Involving Time-Dependent Boundary Regions," Quarterly of Applied Mathematics, v. 26, p. 167, 1968.

9. Irwin, G.R., "Analysis of Stresses and Strains Near the End of a Crack Traversing a Plate," Journal of Applied Mechanics, p. 361, November 1957.

10. American Society for Testing and Materials, Fracture Toughness Testing and Its Applications, pp. 30-82, ASTM, 1964.

11. Naval Postgraduate School - 57Li72011A, Studies Pertaining to Solid Propellant Fracture, by G. H. Lindsey, pp. 17-35, 31 January 1972.

12. JANNAF Interagency Propulsion Committee, JANNAF (formerly ICRPG) Solid Propellant Mechanical Behavior Manual, CPIA Publication No. 21, 1963.

13. Air Force Rocket Propulsion Laboratory, AFRPL-TR-70-105, Application of Fracture Mechanics to Predicting Failures in Solid Propellants, by E. C. Francis et.al., September 1970.

14. Wood, J.E., PhD Thesis in preparation, Aeronautics Department, Naval Postgraduate School, 1972.